DOI: 10.48011/asba.v2i1.1309

# Off-Grid Renewable Generation Control without Energy Storage ⋆

**Fabián L. Forero** * **Ricardo Alzate** * **María A. Mantilla** *
**Rodolpho V. Neves** **

* *Escuela de Ingeniería Eléctrica, Electrónica y de Telecomunicaciones (E3T). Universidad Industrial de Santander (UIS). Bucaramanga. Colombia, (e-mail: fabian.forero1@correo.uis.edu.co; ralzatec@uis.edu.co; marialem@uis.edu.co)*
** *Departamento de Engenharia Elétrica. Universidade Federal de Viçosa (UFV). Minas Gerais. Brasil, (e-mail: rodolpho.neves@ufv.br)*

**Abstract:** This paper addresses the power-sharing of an off-grid generation system including renewable resources without energy storage. Initially, a modified MPPT P&O algorithm is employed to adapt the operation of a photovoltaic array subjected to variations in power demand. Further adjustments are performed to employ the same procedure on a self-excited induction generation extracting wind power. The aforementioned improvements allowed the regulation of DC-link voltages experiencing underloading conditions, restricting their ranges to operational limits of power inverters. Moreover, a parallel combination of both generation units is achieved in terms of a droop power-sharing scheme. Simulation results performed in the SimScape toolbox of MATLAB are presented, confirming the appropriate operation of the off-grid system under variations in demand and power supply conditions. Ongoing work is aimed at the experimental verification on a laboratory prototype for the numerical predictions given.

**Resumen**: Este trabalho trata sobre o compartilhamento de carga de uma microrrede isolada, composta por fontes renováveis sem armazenamento de energia. Inicialmente, um algoritmo MPPT P&O modificado é empregado para adaptar a operação de um arranjo fotovoltaico sujeito a variações de demanda de potência. Ajustes adicionais são feitos para aplicar o mesmo algoritmo MPPT P&O em um gerador eólico de indução auto-excitado. Os ajustes adicionais permitem a regulação da tensão do barramento CC, que será submetido diferentes condições de carga, restringindo os limites operacionais dos inversores. Além disso, uma combinação de operação em paralelo dos geradores fotovoltaico e eólico é realizada, compartilhando cargas utilizando controladores droop. Resultados de simulação obtidos utilizando o toolbox SimScape/MATLAB são apresentados, confirmando a operação apropriada da microrrede isolada sob condições de variação de carga demandada e potência fornecida. A validação dos resultados numéricos deste trabalho ainda está em investigação em um protótipo.

*Keywords:* Droop control; Maximum power-point tracking; Off-grid generation system; Self excited induction generation.

*Palavras-chaves:* Controlador droop; Seguidor do ponto de máxima potência; Microrrede isolada; Gerador de indução auto-excitado.

## 1. INTRODUCTION

Many environmental problems faced nowadays by mankind have their onset in the irresponsible use of fossil fuels and then, new sources of energy must be handled and adapted to reduce the impacts of traditional power generation without sacrificing the demand supply. Accordingly, renewable sources of electric power like wind farms, solar photovoltaic arrays and biomass plants are catching the attention of scientists and engineers worldwide given the increasing necessity of integration for these kind of resources to the main power grid. However, this transition into a decarbonized economy is also a challenge from technological, social and political viewpoints demanding all our attention and effort.

In this context, the new paradigm of electric generation are decentralized and distributed power units combined and managed in terms of the so-called *microgrids*. A microgrid can be operated tied or isolated from the grid. In the first case, the generation system assumes a back-up fashion becoming robust and noncritical. However, isolated (or off-grid) distributed generation systems are interesting solu-

⋆ This work was funded by the Universidad Industrial de Santander under the Project VIE-UIS 2479

tions to supply the demand at non-interconnected areas far from the main power transmission and distribution lines. Such situation is relevant in most Latin American countries where an important amount of the economic activities are developed at rural zones. Moreover, it is unacceptable that people who live surrounded by plenty of natural resources like sun, wind and water, do not have access to electricity.

From a technological perspective, the power management of a microgrid relies on the controlled operation of electronic power converters regulating the energy flowing from sources to loads. The situation becomes challenging when it involves renewable resources of random availability. Hence, in order to achieve a maximum extraction of power from renewable sources, control techniques based on the maximum point tracking principle (MPPT) have been proposed massively in the literature (Eltamaly and Abdelaziz (2020)). Under such schemes the load will be fully supplied and the excess of power can be stored for further use. However, energy storage is not a clever choice regarding the size, cost and environmental (disposal) restrictions appearing on certain applications. In other words, a distributed system without energy storage constitutes a cheaper, simpler and smaller solution for a power generation unit fitting demand and budget conditions at rural zones of development countries.

On the other hand, energy management of power grids has been traditionally solved using the *droop* technique for power sharing (Peng et al. (2019)). Under static mode (i.e. non-economic dispatch), the *droop* control will schedule the references for the primary level loops on a hierarchic control scheme. However, this upper level control acts detached from the MPPT routines involving maximum extraction of power from the renewable sources, causing inconveniences at the DC link under power excess and consequently altering the operation of inverters and the quality of power delivered to the system load (He et al. (2011)). Actually, inappropriate DC link voltages can even destroy the inverters, implying waste of time and money for recovering the system.

Inspired by the aforementioned ideas, this paper proposes a modified MPPT algorithm adapting the power generation to load requirements, under isolated operation without energy storage. The proposed scheme involves two renewable sources (a photovoltaic array and a rotative self-excited induction generator) combined in parallel under *droop* power sharing.

## 2. GENERAL DESCRIPTION OF THE SYSTEM

The scheme identifying main blocks for the off-grid generation system, without energy storage, is presented in Figure 1. As it can be seen, the system is composed by two generation units operating in parallel to feed a common load of 1.2 kW (purely resistive impedance). Specific details for each generator, including circuit structure and internal control loops, will be addressed as follows.

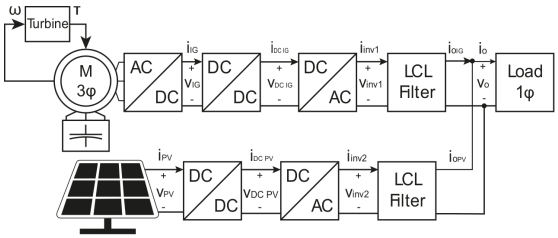


Figure 1. Block diagram for the off-grid generation system.

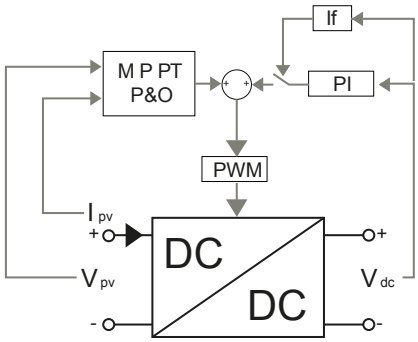


Figure 2. Modified P&O algorithm to regulate the DC link voltage at the photovoltaic unit.

### *2.1 Photovoltaic unit*

Essentially, the photovoltaic generator is composed of an array of 1 kW coupled to a boost power converter, transforming 160 VDC (at nominal conditions of irradiance and temperature) into 450 VDC, as the DC link voltage applied at the input of a full-bridge inverter. The output of the inverter is connected to the load at a single phase AC bus of 120 VAC / 60 Hz. Specific circuit parameters for the boost converter and the power inverter are detailed in Forero-Ordóñez et al. (2020).

In terms of power flow control, the commutation pattern of the inverter is built-up by a SPWM module with a double-loop PI resonant controller regulating the output voltage to the desired nominal value. On the other hand, the boost converter is subjected to a P&O (Perturb and Observe) algorithm extracting the maximum power from the photovoltaic array (Xu et al. (2020)). However, as the system is conceived without storage, an interesting situation is arising when the available input power exceeds the load demand. Under such situation a traditional P&O algorithm will continue tracking the maximum power point (MPPT) increasing the DC link voltage above safe limits. In order to avoid that, a combination of PI regulation and P&O MPPT is proposed as sketched in Figure 2. In such an approach, the PI loop will be activated just after detecting the DC link voltage is above its nominal value. Then, after correcting it, the extraction of power from the PV source continuous with the P&O action. A deeper discussion on this method can be found in Forero-Ordóñez et al. (2020).

### *2.2 Induction generation unit*

In complement to the photovoltaic unit, the scheme includes a rotative generator of the squirrel-cage induction

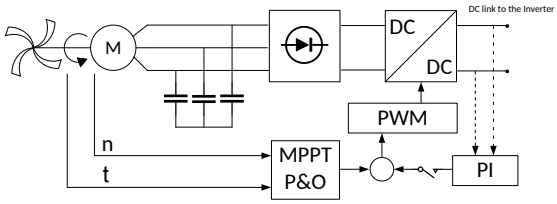


Figure 3. SEIG with DC link voltage regulation.

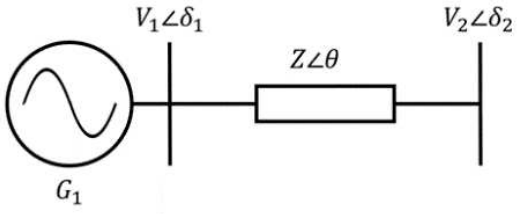


Figure 4. Generator linked to a bar of an electric grid.

type. In this case, a self-excited generation unit is configured as presented in Figure 3 for a three phase machine of 2 HP / 1700 RPM. Self-excited induction generators (SEIG) are feasible renewable sources for low power applications involving conversion of wind or water flows into motion (Murthy and Ahuja (2010)). In this case the modified P&O MPPT algorithm was also applied to adapt the power generated to the load demand. However, instead of reacting to the input (voltage and current) variables of the boost converter, the algorithm performed an exploration of the torque($\tau$)-velocity($n$) curve of the SEIG (Manaullah et al. (2014); Costa and Sales (2018)).

Once the DC-link has been regulated by the modified MPPT P&O and adapted to the rotation machine, the power inverter creates the sinusoidal output voltage replicating the circuit described for the photovoltaic unit.

## 3. GRID CONFIGURATION

The parallel combination of both generation units is performed by a power-sharing *droop* technique (Chandorkar et al. (1993)). To understand the principle of the method let us consider the simple situation depicted in Figure 4 where a generator $G_1$ of voltage $V_1\angle\delta_1$ is connected to a bar of voltage $V_2\angle\delta_2$ through an impedance $Z\angle\theta$.

The calculation for mathematical expressions involving the power delivered from the generator to the grid, are presented in the *Appendix* at the end of the manuscript. In accordance, the following comments can be stated:

- The power generated by the system under study is active (i.e. real), given the resistive features assumed on the load side;
- From (A.1), the maximum value for the instantaneous active power $P$ corresponds to $\Lambda = \frac{|V_1||V_2|}{X}$;
- The magnitude of $P$ depends on the phase deviation $\Delta\delta = (\delta_2 - \delta_1)$ and then $\sin(\Delta\delta) \approx \Delta\delta$ for $\Delta\delta \to 0$.

Therefore:

$$\begin{aligned} P &\approx \Lambda\, \Delta\delta \\ &\approx \Lambda\, \Delta\omega\, t \\ &\approx (\Lambda\, t)\, \Delta\omega \\ &\approx m\Delta\omega, \end{aligned} \tag{1}$$

given $\delta = \omega t$ for a periodic $t$. The latter represents a linear relationship between $P$ and $\Delta\delta$ with a further coordinate change to $\Delta\omega$, as depicted in Figure 5.

Hence, provided $V_1$, $V_2$ and $X$, the values for $\Lambda$ and $\Gamma$ (a power corresponding to $\Delta\delta \to 0$) can be calculated from (A.1). Then for the same $\Gamma$, the slope $m$ will be determined from (1) for a desired range $\Delta\omega$.

In particular, assuming $V_1 = 174.5$ VAC and considering the output constraint $V_2\angle\delta_2 = 170\angle(2\pi \times 60)\,t$, the parameters for the droop power-sharing were selected as listed in Table 1.

Table 1. Parameters for the droop power-sharing scheme

| Parameter | Description | Value |
|---|---|---|
| $X_{PV}$ | Line impedance of PV | 7 mH |
| $\Lambda_{PV}$ | Maximum power at PV | 11.24 kW |
| $\Delta\delta$ | Phase deviation | $1 \times 10^{-2}$ rad |
| $\Gamma_{PV}$ | Power at PV for $\Delta\delta \to 0$ | 112.4 W |
| $\Delta\omega$ | Frequency deviation | $2\pi \times 10^{-4}$ rad/s |
| $m_{PV}$ | Slope for PV | $1.79 \times 10^5$ |
| $X_{IG}$ | Line impedance of SEIG | 9 mH |
| $\Lambda_{IG}$ | Maximum power at SEIG | 8.74 kW |
| $\Gamma_{IG}$ | Power at SEIG for $\Delta\delta \to 0$ | 87.4 W |
| $m_{IG}$ | Slope for SEIG | $1.39 \times 10^5$ |

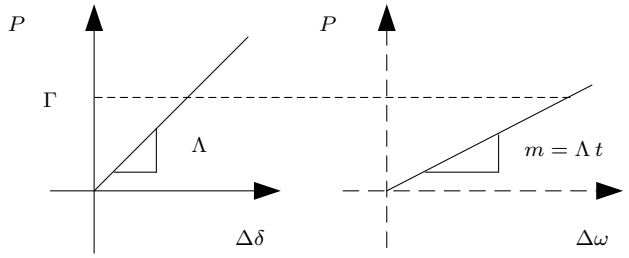


Figure 5. Linear approximation between $P$, $\Delta\delta$ and $\Delta\omega$.

On the other hand, the output constraint implies:

$$\Delta\omega = \omega_2 - \omega_1 = (2\pi \times 60) - \omega_1 = 120\pi - \omega_1,$$

allowing to write from (1):

$$P \approx m\,(120\pi - \omega_1) \quad \Rightarrow \quad \omega_1 = 120\pi - \frac{P}{m}. \tag{2}$$

Then, if $P_{PV}$ represents the power provided by the photovoltaic unit and $P_{IG}$ the contribution of the SEIG, the synchronization requirements of the isolated microgrid impose the following condition for connection:

$$\frac{P_{PV}}{m_{PV}} = \frac{P_{IG}}{m_{IG}} \quad \Rightarrow \quad \frac{m_{IG}}{m_{PV}} = \frac{P_{IG}}{P_{PV}},$$

defining the proportion or amount of power-sharing provided by the *droop*.

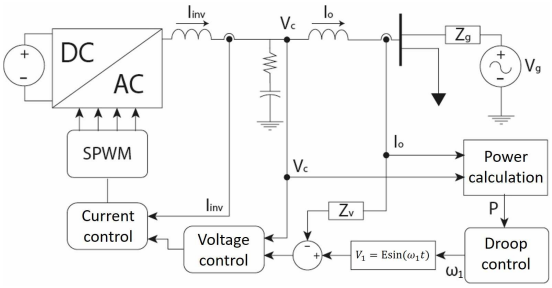


Figure 6. Illustration for *droop* branch applied on a single inverter.

Finally, a virtual impedance $Z_v$ is added to the transmission line, such that:

$$X = X_0 + Z_v,$$

with $X_0$ representing the physical reactance of the line. Figure 6 illustrates the detail for the *droop* topology configured at each power inverter, as a single contribution to the load bus.

In summary, the active power $P$ is measured from the load. Then, the *droop* will calculate from (2) the frequency $\omega_1$ required to construct $V_1$. This frequency value is further employed as the carrier of the SPWM for the power inverter. Finally, the reference of the voltage loop (corresponding to the desired voltage $V_2$ at the load bus) is synthesized by removing from $V_1$ the voltage drop of the virtual impedance.

It is important to notice that the approach proposed here corresponds with a *droop* control applied to an inverter acting as a voltage source. This is slightly different to other approaches employing current sources. An interesting discussion of the topic can be found in (Guerrero et al. (2009)).

## 4. SYSTEM OPERATION

In order to verify the operation of the off-grid generation system without energy storage, numerical simulations were performed in MATLAB employing the *SimScape* toolbox. In doing so, a functional block of wind turbine configured with default parameters was employed to model the mechanical conversion from wind power into rotational motion as well as a PV array to convert the solar irradiance into electrical power.

The simulation scenario included a starting transient with zero initial conditions, verifying the following sequence of events: 1) at $t = 0$ $s$ the photovoltaic generator ($G_1$) and the SEIG ($G_2$) start their operation disconnected from the load bus; 2) at $t = 0.4$ $s$ the rotational speed of the SEIG reaches the synchronous value starting the power generation; 3) at $t = 1$ $s$ a load demand of 900 W is connected to $G_1$; 4) at $t = 2$ $s$ the load is shared among both generators by a direct parallel connection; 5) at $t = 3.5$ $s$ the load demand increases to 1.2 kW;6) at $t = 4.5$ $s$ the wind profile is varied from 12 $m/s$ to 11 $m/s$ following a linear pattern; 7) at $t = 6.5$ $s$ the solar irradiance is varied from $1000W/m^2$ to $900W/m^2$ following a linear pattern.

The corresponding results are depicted in Figs. 7-10. As it can be noticed, despite the several changes applied to load and supply powers, the DC link voltages tend to be regulated to the desired nominal values of 450 VDC for $G_1$ (see Figure 7(a)) and 500 VDC for $G_2$ (see Figure 7(b)). In particular, the effects of disturbances applied on the irradiance and wind flows, can be observed in detail by the waveforms captured for the input voltages at the boost converter stages shown in Figure 8(a) for the photovoltaic generator and in Figure 8(b) for the SEIG. The dynamical behavior experienced unveils the effectiveness of the modified MPPT P&O algorithm proposed, not only in terms of fast and convergent transients but also accomplishing desired steady-state conditions.

It is also verified from Figure 9 the power-sharing performed among the generation units, allowing to provide the required power demand at the load along the different practical scenarios considered, while keeping acceptable proportion rates of contributions during the simulation interval, confirming the performance expected by calculations on the droop control technique.

A better detail of the latter can be observed from the power profiles at each generator. In Figure 10(a), the power of the PV unit is depicted, showing by a square the scenario for $t < 2$ $s$, by a circle the scenario for $2 \leq t < 3.5$ $s$ and by an asterisk the scenario for $t \geq 3.5$ $s$. Also, Figure 10(b) presents for the SEIG equivalent results for $2 \leq t < 3.5$ $s$ with a square, for $3.5 \leq t < 4.5$ $s$ with a circle and for $t \geq 4.5$ $s$ with an asterisk. All of these confirming the operation of the system regulated at the required power demand.

## 5. CONCLUDING REMARKS

This paper presented the configuration and power flow control of an off-grid generation scheme without energy storage, subjected to variations in load demand and power supplies. In particular, a modified MPPT P&O algorithm was employed to adapt the power extraction to the operation point, given the excess of power during underloading conditions. In this context, an interesting contribution of the manuscript relies on the connection created between a droop power-sharing control and the DC link regulation, assuring proper operation of the inverter to supply the required demand without increasing the safe limits of voltages at their input. Simulation results have shown an appreciable performance of the modified MPPT algorithm for two different types of renewable energy sources, which gives promising application of the proposed method into distributed generation schemes at low power levels. Ongoing work is aimed at the experimental verification in a laboratory prototype for the numerical predictions presented here.

## REFERENCES

Chandorkar, M.C., Divan, D.M., and Adapa, R. (1993). Control of parallel connected inverters in standalone

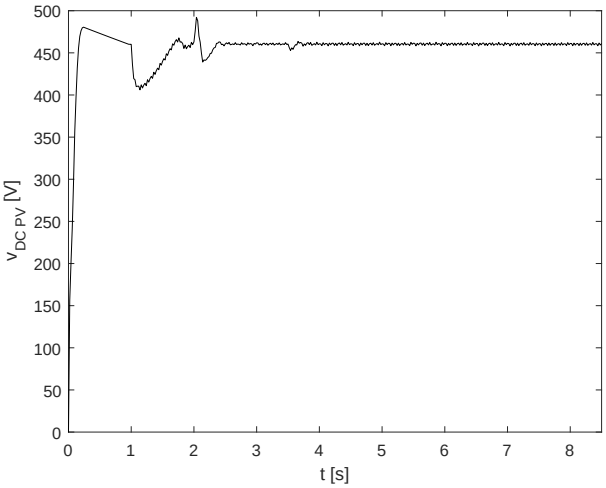


(a) $V_{DC\ PV}$

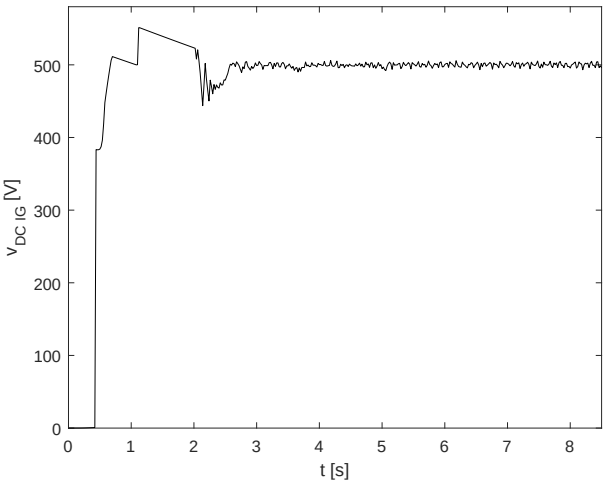


(b) $V_{DC\ IG}$

Figure 7. DC link voltages.

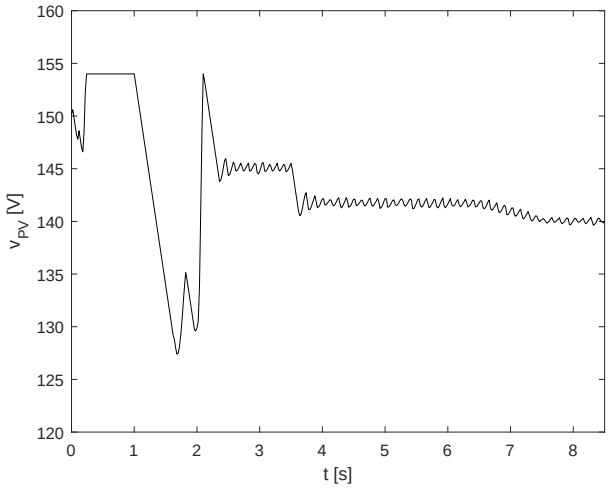


(a) $V_{PV}$

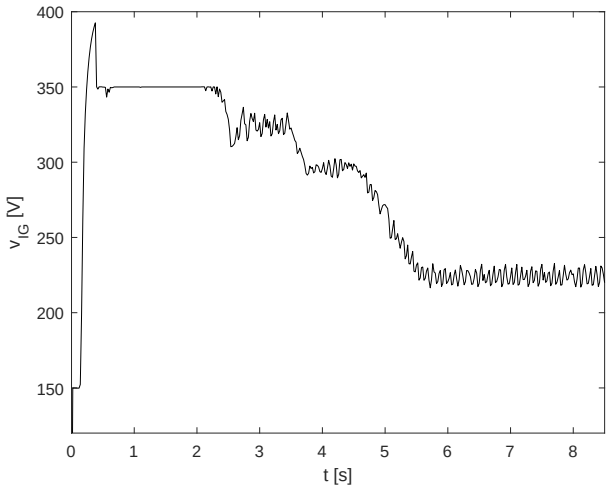


(b) $V_{IG}$

Figure 8. Voltages at the input of each boost converter.

AC supply systems. *IEEE Transactions on Industry Applications*, 29(1), 136–143.

Costa, A. and Sales, L. (2018). Rastreamento da máxima potência de turbinas eólicas baseadas em máquina de induçao com motor em gaiola através do controle por escorregamento com fluxo estatorico. In *XXII Congresso Brasileiro de Automática*.

Eltamaly, A.M. and Abdelaziz, A.Y. (2020). *Modern maximum power point tracking techniques for photovoltaic energy systems*. Springer.

Forero-Ordóñez, F., Mantilla-Villalobos, M.A., and Alzate-Castaño, R. (2020). An improved method for power tracking on isolated PV systems without energy storage. In *International Symposium of Electric Power Quality - SICEL*, to appear.

Guerrero, J.M., Vasquez, J.C., Luna, A., Rodriguez, P., and Teodorescu, R. (2009). Adaptive droop control applied to voltage-source inverters operating in grid-connected and islanded modes. *IEEE Transactions on Industrial Electronics*, 56(10), 4088–4096.

He, F., Zhao, Z., Yuan, L., and Lu, S. (2011). A DC-link voltage control scheme for single-phase grid-connected PV inverters. In *2011 IEEE Energy Conversion Congress and Exposition*, 3941–3945.

Manaullah, A.K., Sharma, H., and Ahuja, A. (2014). Performance comparison of DFIG and SCIG based wind energy conversion systems. In *IEEE Innovative Applications of Computational Intelligence on Power*.

Murthy, S.S. and Ahuja, R.K. (2010). A novel solid state voltage controller of three phase self excited induction generator for decentralized power generation. In *2010 International Conference on Power, Control and Embedded Systems*, 1–6.

Peng, Z., Wang, J., Bi, D., Wen, Y., Dai, Y., Yin, X., and Shen, Z.J. (2019). Droop control strategy incorporating coupling compensation and virtual impedance for microgrid application. *IEEE Transactions on Energy Conversion*, 34(1), 277–291.

Xu, L., Cheng, R., and Yang, J. (2020). A new MPPT technique for fast and efficient tracking under fast varying solar irradiation and load resistance. *International Journal of Photoenergy*, 2020, 1–18.

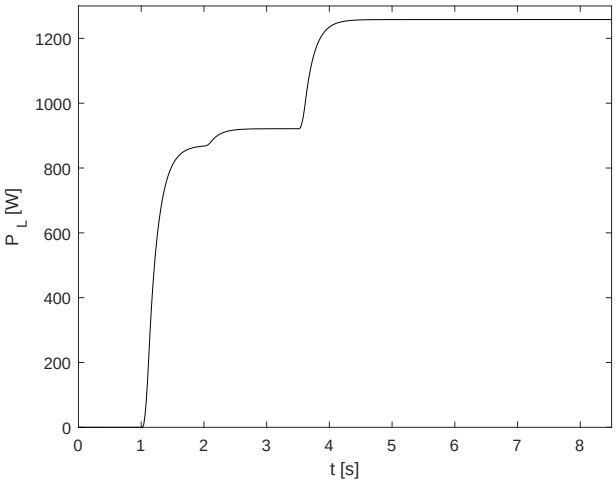


(a) Load power

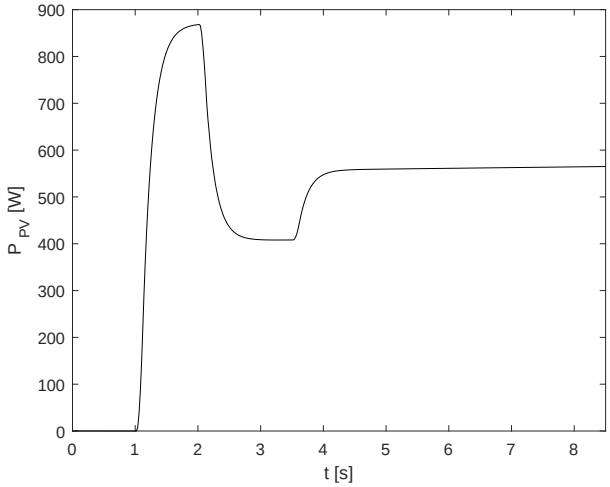


(b) Power provided by PV unit

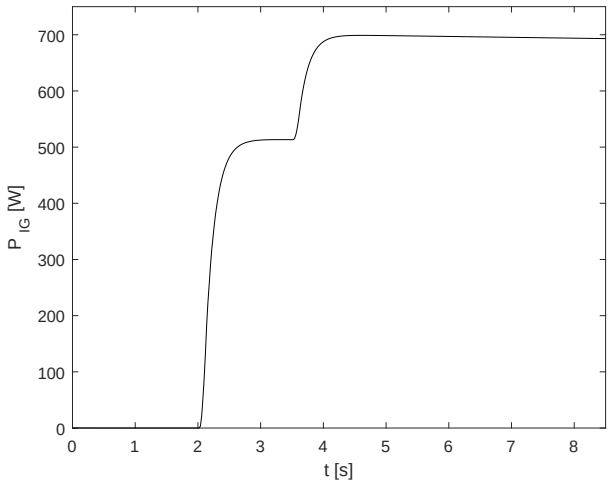


(c) Power provided by SEIG unit

Figure 9. Power sharing for the off-grid generation scheme subjected to disturbances.

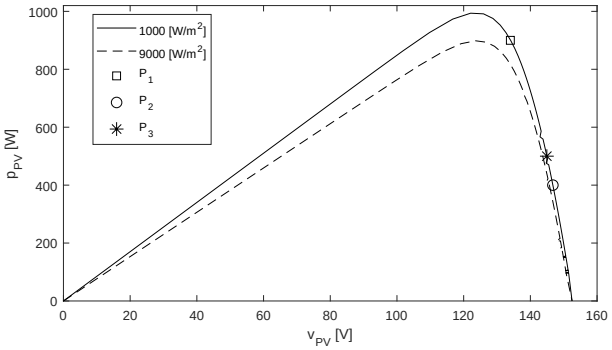


(a) PV unit

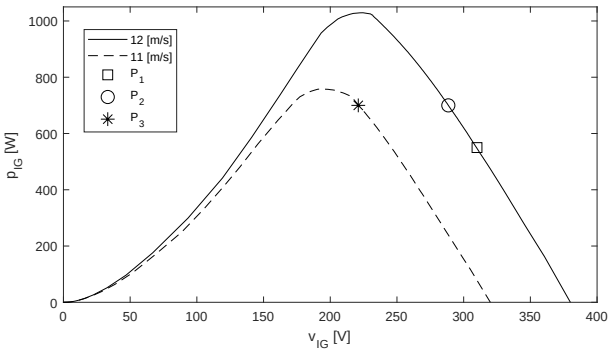


(b) SEIG unit

Figure 10. Power profiles showing operational points.

## Appendix A. CALCULATION FOR POWER DELIVERED TO THE GRID FROM A GENERATOR

The apparent power delivered from the generator to the bar in Figure 4, can be calculated as follows:

$$
\begin{aligned}
S &= V_1 \times I^* \\
&= |V_1| e^{j\delta_1} \times \left( \frac{|V_1| e^{j\delta_1} - |V_2| e^{j\delta_2}}{|Z| e^{j\theta}} \right)^* \\
&= \frac{|V_1|^2}{|Z|} e^{j\theta} - \frac{|V_1||V_2|}{|Z|} e^{j(\delta_1 - \delta_2 + \theta)} \\
&= \frac{|V_1|^2}{|Z|} \left( \cos(\theta) + j \sin(\theta) \right) - \\
&\quad \frac{|V_1||V_2|}{|Z|} \left( \cos(\delta_1 - \delta_2 + \theta) + j \sin(\delta_1 - \delta_2 + \theta) \right) \\
&= \left( \frac{|V_1|^2}{|Z|} \cos(\theta) - \frac{|V_1||V_2|}{|Z|} \cos(\delta_1 - \delta_2 + \theta) \right) + \\
&\quad j \left( \frac{|V_1|^2}{|Z|} \sin(\theta) - \frac{|V_1||V_2|}{|Z|} \sin(\delta_1 - \delta_2 + \theta) \right) \\
&= P + jQ,
\end{aligned}
$$

being $P$ the active and $Q$ the reactive, components of power.

Moreover, if $Z$ is a purely inductive transmission line of reactance $X$ then $\theta = \frac{\pi}{2}$ and the expressions can be simplified to:

$$
\begin{aligned}
P &= \left( \frac{|V_1|^2}{X} \cancel{\cos\left(\frac{\pi}{2}\right)}^{0} - \frac{|V_1||V_2|}{X} \cos\left(\delta_1 - \delta_2 + \frac{\pi}{2}\right) \right) \\
&= \left( -\frac{|V_1||V_2|}{X} \sin\left(\delta_1 - \delta_2\right) \right) \\
&= \left( \frac{|V_1||V_2|}{X} \sin\left(\delta_2 - \delta_1\right) \right), \qquad \text{(A.1)}
\end{aligned}
$$

after exploiting the odd feature of the sine function, and:

$$
\begin{aligned}
Q &= \left( \frac{|V_1|^2}{X} \cancel{\sin\left(\frac{\pi}{2}\right)}^{1} - \frac{|V_1||V_2|}{X} \sin\left(\delta_1 - \delta_2 + \frac{\pi}{2}\right) \right) \\
&= \left( \frac{|V_1|^2}{X} - \frac{|V_1||V_2|}{X} \cos\left(\delta_1 - \delta_2\right) \right) \\
&= \left( \frac{|V_1|^2}{X} - \frac{|V_1||V_2|}{X} \cos\left(\delta_1 - \delta_2\right) \right).
\end{aligned}
$$